

An ultra low power CMOS pA/V transconductor and its application to wavelet filters

Peterson R. Agostinho · Sandro A. P. Haddad ·
Jader A. De Lima · Wouter A. Serdijn

Received: 26 November 2007 / Revised: 7 May 2008 / Accepted: 2 June 2008 / Published online: 21 June 2008
© Springer Science+Business Media, LLC 2008

Abstract Two compact ultra low-power CMOS triode transconductor topologies denoted VLPT- g_m and Delta- g_m are proposed. In both circuits, input transistors are kept in the triode region to benefit from the lowest g_m/I_D ratio. This allows achieving a small-signal transconductance g_m down to hundreds of pA/V, making such transconductors attractive for the synthesis of g_m -C filters with cut-off frequencies in the range of Hz and sub-Hz. The g_m value is adjusted by a well defined aspect-ratio (W/L) and drain-source voltage V_{DS} , the latter a replica of the tuning voltage V_{TUNE} imposed as drain-source voltage of input devices. VLPT- g_m reaches a minimum g_m of 1 nA/V, whereas Delta- g_m exhibits a g_m as low as 400 pA/V. Input-referred noise spectral density is typically $12.33 \mu\text{V}/\text{Hz}^{1/2}$ @ 1 Hz and $93.75 \mu\text{V}/\text{Hz}^{1/2}$ @ 1 Hz for VLPT- g_m and Delta- g_m , respectively. In addition, setting their g_m equal to 1 nA/V and arranging them as first-order lossy integrators, Delta- g_m presents higher bandwidth with respect to VLPT- g_m . Cut-off frequencies are 1.33 kHz and 24 kHz for VLPT- g_m and Delta- g_m integrators, respectively. Finally, as an application example, both transconductors were used as building blocks to realize a 6th-order wavelet g_m -C filter. For both approaches, THD was kept below 1% for

signal swings up to 200 mV_{pp}. The design complies with a 1.5 V supply and a 0.35 μm CMOS process and features an overall power consumption of 51 and 114 nW, respectively for VLPT- g_m and Delta- g_m filters.

Keywords Low-frequency filters · CMOS transconductors · g_m -C filter · Wavelet filter

1 Introduction

In the field of medical electronics, active filters with large time constants are often required to attain very low cutoff-frequencies, in Hz and sub-Hz ranges. Since passive filters demand bulky capacitors and/or resistors to implement such time constants, they are rarely employed. Owing to their low-voltage low-power (LVLP) compatibility, g_m -C structures are a natural choice to perform the desired filtering characteristic, as long as very-low values of small-signal transconductance g_m , typically a few nA/V or less, can be achieved.

Previous works on LVLP CMOS techniques for obtaining a very-low transconductance essentially combine different strategies such as voltage attenuation, source degeneration and current splitting [1–4]. The intrinsic input-voltage attenuating properties of floating-gate and bulk-driven techniques are exploited in [1]. The former solution demands nonetheless a double-poly fabrication process, whereas the latter implies a finite input-impedance transconductor and lack of precision, as the bulk transconductance g_{mb} is very process-dependent. In the source-degeneration scheme presented in [2], a triode-biased transistor acts as a simple voltage-controlled resistor. Matching is a crucial problem in current splitting, since a large number of unity-cell transistors compose the current

P. R. Agostinho
Electrical Engineering Department, Technological Institute
of Aeronautics, Sao Jose dos Campos, SP, Brazil

P. R. Agostinho · S. A. P. Haddad · W. A. Serdijn
Electronics Research Laboratory, Faculty of Electrical
Engineering, Delft University of Technology, Delft,
The Netherlands

S. A. P. Haddad · J. A. De Lima (✉)
Brazil Semiconductor Technology Center, Freescale
Semiconductor, 13069-380 Campinas, SP, Brazil
e-mail: jader.delima@freescale.com

mirrors to implement very-high division factors. In [3], a downscaling factor of 40,000 is proposed, and in order to have all devices operating in strong-inversion for an improved mirroring, a bias current of 15 μA is required. Because the final current of around 400 pA is well above leakage current levels, a more predictable transconductance is obtained, at the expense of power consumption. Conversely, a smaller division factor of 784 and a lower bias current are defined in [4], reducing the final current to only a few pA, which implies a less accurate transconductance.

Even though working either in weak, moderate or strong inversion, the transconductor input-transistor is always kept in saturation in the above-mentioned techniques. However, the lowest g_m/I_D ratio is obtained in strong-inversion triode-region (SI-TR), as discussed in Sect. 2. Although this feature compromises the use of triode-transconductors in very-high frequency g_m -C filters, it turns out attractive when operation in the lower end of the frequency spectrum is devised. In [5], a low- g_m pseudo-differential transconductor based on a four-quadrant multiplication scheme is presented, in which the drain voltage of a triode-operating transistor follows the incoming signal. Nevertheless, because triode operation needs to be sustained, the input-signal swing is rather limited. Moreover, this solution only applies to balanced structures. Although triode-transconductors, in which the signal is directly connected to the input-transistor gate, have been successfully employed in high-frequency g_m -C filters [6, 7], its potential for very-low frequency filter designing has been scarcely exploited in the open literature [8].

This paper presents two compact topologies for ultra low-power transconductors, as improvements of the basic concept introduced in [9]. These approaches are named VLPT- g_m (Very Low-Power Triode transconductor) and Delta- g_m that features values of g_m in the range of few nA/V and hundreds of pA/V, respectively. Subsequently, an implementation of the wavelet transform with a Gaussian wavelet (*gaussI*) in an ultra low-power environment, based on the proposed transconductors, is considered. Low-power analog realization of the continuous wavelet transform enables its application in vivo, e.g. in pacemakers and IECG recorders.

Thus far, analog implementation of the continuous low-frequency wavelet transform by means of a so-called wavelet filter has employed both bipolar and CMOS Dynamic-Translinear (DT) circuits [10], which become difficult to integrate when designing very low-frequency filters. As an example, for $g_m = 1$ nA/V, VLPT- g_m needs to be biased with a quiescent current I_Q of around 300 pA. To achieve the same time constant, while keeping the bias current value, the DTL circuit would require an increase of 12.6 times in capacitor values, unacceptably enlarging the

die size. Alternatively, to maintain the same capacitor, it would be necessary to decrease I_Q to 25 pA. However, an accurate current source with such an ultra-low value is not attainable on practice due to leakage mechanisms and process spread. Moreover, the resulting DTL filter would be overly noisy.

The paper is organized as follows: Sect. 2 describes both LVLP triode transconductors circuits. Design and implementation of the wavelet filter are discussed in Sect. 3. Simulation data that validate the circuit performance and its tuning capability are presented in Sect. 4. Conclusions and final remarks are summarized in Sect. 5.

2 Transconductors description

2.1 Why strong-inversion triode-region?

The g_m/I_D ratio is listed in Table 1, for distinct MOSFET regions: SI-TR, weak-inversion saturation (WI-S) and strong-inversion saturation (SI-S). The gate-overdrive voltage is $V_{GO} = V_{GS} - V_{TO}$, where V_{TO} is the threshold voltage. U_T and n are the thermal voltage and the weak-inversion slope factor, respectively. As it can be noted, for a source-grounded device and V_{DS} small, the lowest g_m/I_D occurs for SI-TR operation, as V_{GO} can be set much higher than nU_T .

2.2 VLPT- g_m Transconductor

The schematic of VLPT- g_m transconductor is shown in Fig. 1. With respect to the circuit presented in [9], a common-gate stage M_{3A} - M_{3B} is introduced into the loop of the auxiliary voltage amplifier. The transconductor input-referred equivalent noise and output swing remain practically the same. However, there is a significant improvement in the auxiliary amplifier open-loop gain, and consequently, on the transconductor output resistance. Denoting A_{L1} and A_{L2} as the auxiliary amplifier open-loop gain voltage in the original circuit in [9] and VLPT- g_m , respectively, one has

$$A_{L1} \cong g_{m2}r_{ds2} \quad (1)$$

$$A_{L2} \cong g_{m2}r_{ds2}g_{m3}r_{ds3} \quad (2)$$

Input transistors M_{1A} - M_{1B} have their drain voltages regulated by an auxiliary amplifier that comprises M_{2A} - M_{2B} , M_{3A} - M_{3B} , M_{4A} - M_{4B} and bias current sources M_{7A} -

Table 1 MOSFET g_m/I_D ratio in different operation regions

	WI-S	SI-TR	SI-S
$\frac{g_m}{I_D}$	$\frac{1}{nU_T}$	$\frac{1}{V_{GO} - \frac{nV_{DS}}{2}}$	$\frac{2}{V_{GO} - nV_s}$

$$i_{OUT} = (i_{1B} + i_{1D}) - (i_{1A} + i_{1C}) \tag{4}$$

where i_{1A} , i_{1B} , i_{1C} and i_{1D} are small-signal currents flowing through M_{1A} , M_{1B} , M_{1C} and M_{1D} , respectively. Considering M_{1A} and M_{1B} to be ideally matched, as well as M_{1C} and M_{1D} , one has

$$i_{OUT} = \frac{V_{in}}{2} g_{m1D} \Delta + \frac{V_{in}}{2} g_{m1C} \tag{5}$$

$$i_{OUT} = \Delta g_{m1C,D} V_{IN} \tag{6}$$

and therefore

$$g_{m_Delta} = \Delta g_{m1C,D} = \Delta \beta_{1C,D} V_{TUNE} \tag{7}$$

so that g_{m_Delta} corresponds to a fraction of g_{m_VLPT} . As a consequence, a Delta- g_m transconductor represents a better alternative as compared to a VLPT- g_m counterpart to attain ultra-low g_m values.

3 Wavelet filter design

Wavelet literally means small wave. Wavelet analysis is performed using a prototype function called the wavelet base, which decomposes a signal into components appearing at different scales (or resolutions). A wavelet filter performs a wavelet transform when its impulse response corresponds with the desired wavelet base [10]. There are several types of well-defined wavelet bases, for instance, Gaussian, Morlet and Daubechies. Depending on the application (and the properties of the wavelet transform), one may be preferred over others.

Unfortunately, a linear differential equation having a pre-defined desired impulse response does not always exist. Hence, one is obliged to use a suitable approximation method, the topic of the next section. In this paper, only the Gaussian wavelet filter will be presented, but several wavelet bases can also be approximated using the proposed approach [10].

There are several techniques that are frequently used to achieve the best approximation possible. Nonetheless, one of the most important aspects of an analog filter synthesis is that the approximating function must lead to a physically realizable network which is dynamically stable.

3.1 L_2 approximation

As mentioned in [10], approximation methods should be applied to obtain the required transfer function of a wavelet filter’s impulse response. A method which has proven to be successful is provided by the Padé approximation of the Laplace transform of the impulse response $h(t)$ of the filter [10]. Another alternative to find a suitable wavelet base approximation can be provided by the theory of L_2 approximation [12].

The advantage of the L_2 method over the Padé approximation is that the L_2 approximation offers a more

global approximation, i.e., not concentrating on one particular point (in the Laplace domain). Also, the fit can be performed directly in the time domain, yielding good control and easy interpretation of the optimization criteria. The L_2 approximation technique is based on minimizing the least-mean-square-error. In this scheme the error integral, which is the difference between the wavelet function $\psi(t)$ and its approximation $h(t)$, is defined by

$$\varepsilon_{L2} = \int_0^\infty (\psi(t) - h(t))^2 dt \tag{8}$$

In order to derive the L_2 approximation, we first express the impulse response (in the time domain) of a general filter. After that, the error ε_{L2} is minimized with respect to the poles and zeros of the wavelet filter. For the generic situation of stable systems with distinct poles, $h(t)$ may typically have the following form [12]

$$\begin{aligned} h(t) &= \sum_{i=1}^n A_i e^{P_i t} \\ &= \sum_{i=1}^k c_i e^{P_i t} + c_{k+1} e^{P_{k+1} t} \sin(p_{k+2} t) \\ &\quad + c_{k+2} e^{P_{k+1} t} \cos(p_{k+2} t) + \dots + c_{n-1} e^{P_{n-1} t} \sin(p_n t) \\ &\quad + c_n e^{P_{n-1} t} \cos(p_n t) \end{aligned} \tag{9}$$

where A_i and P_i can be real or complex numbers; c_i and p_i are real numbers, representing the impulse response function $h(t)$ as a linear combination of damped exponentials and exponentially damped harmonics. k corresponds to the number of real poles and n is the order of the filter.

Then, given the explicit form of a wavelet base $\psi(t)$ and the approximated impulse response $h(t)$, the L_2 -norm of the difference $\psi(t)-h(t)$ can now be minimized in a straightforward way using standard numerical optimization techniques and software. The most direct way to find the minimum of Eq. 9 is by computation of all partial derivatives of ε_{L2} with respect to A_i and P_i and setting them equal to zero, namely

$$\frac{\partial \varepsilon_{L2}}{\partial A_i}, \frac{\partial \varepsilon_{L2}}{\partial P_i} = 0 \quad \text{for } i = 1 \dots n \tag{10}$$

The wavelet base approximation using the proposed L_2 approach is given in Fig. 4, where the first derivative of a Gaussian wavelet base (*gauss1*) has been approximated using the corresponding 6th-order transfer function

$$H(s) = \frac{0.16s^4 - 8.32s^3 + 6.64s^2 - 139s}{s^6 + 5.9s^5 + 30.5s^4 + 83.1s^3 + 163s^2 + 176s + 93.3} \tag{11}$$

3.2 State-space filter implementation

To meet low-power low-voltage requirements, the state-space description of the filter has been optimized with

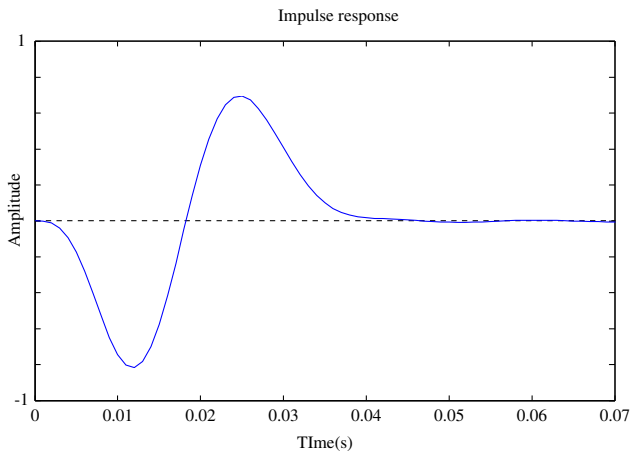


Fig. 4 L_2 approximation of the first derivative of Gaussian

respect to dynamic range, sparsity and sensitivity [10]. The filter design that follows is based on an orthonormal ladder structure and employs the Delta- g_m transconductor described in the previous section as the basic building block of the filter diagram in Fig. 5. In order to obtain the corresponding g_m -C filter realization, one first needs to map the state-space coefficients on respective g_m values. From Eq. 3, one can vary the value of g_m by either changing $(W/L)_1$ or the drain-source voltage (V_{TUNE}) of transistor M_1 . Nevertheless, owing to additional bias stages required to determine different filter coefficients, the realization of several V_{TUNE} generators would increase the power consumption by a factor of $(n - 1)P_{Bias}$, where n is the number of implemented coefficients and P_{Bias}

represents the power consumption of the bias stage. Therefore, the option of adjusting g_m by re-sizing $(W/L)_1$ was adopted.

4 Simulation results

As a proof of concept, a wavelet Gm-C filter was simulated using parameters of a standard 0.35 μm CMOS IC fabrication process and Bsim3v3 models. Two different filter versions, based on VLPT- g_m and Delta- g_m circuits, have been designed to operate from a 1.5-V supply voltage V_{DD} , to which tuning voltage V_{TUNE} is referred. For a typical g_m of 4 nA/V, transistor sizing and bias currents are listed in Tables 2 and 3, respectively.

To implement the different coefficients of the state-space representation, the width of input transistors M_{1A} and M_{1B} was properly adjusted, whereas keeping V_{TUNE} fixed to 20 mV. Figure 5 shows the block diagram of the wavelet filter and the value of g_m for each transconductor. Analysis of g_m with respect to input voltage and tuning was also realized for both VLPT- g_m and Delta- g_m . For a 1 k Ω -load at the transconductor output, fixing V_{in}^- to a bias voltage and sweeping V_{in}^+ , the g_m dependence on tuning for $10\text{ mV} \leq V_{TUNE} \leq 50\text{ mV}$ is plotted in Fig. 6, where $V_{in} = V_{in}^+ - V_{in}^-$. Transconductance spans from 1 to 5 nA/V and remains almost constant in the triode region for the same V_{TUNE} , whereas linearly scaling with this voltage.

The transconductor frequency response as an integrator is also analyzed. For an integrating capacitor of 20 pF and

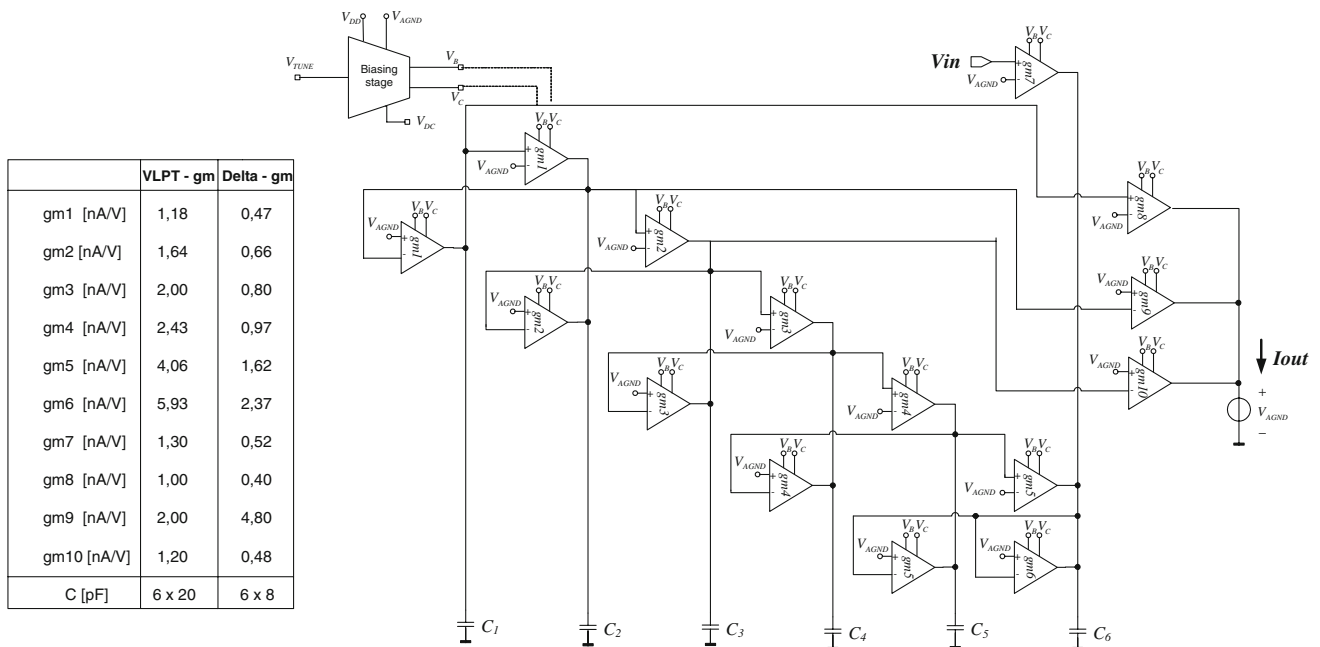


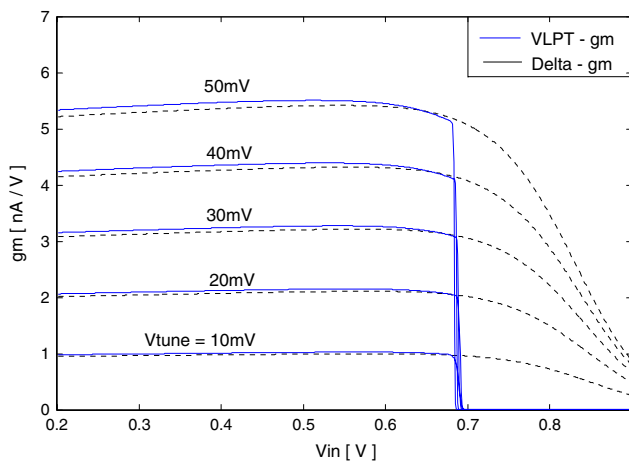
Fig. 5 Block diagram of 6th-order Gauss1 wavelet filter

Table 2 Transconductor transistor sizing for $g_m = 4 \text{ nA/V}$

	W/L ($\mu\text{m}/\mu\text{m}$) VLPT- g_m	W/L ($\mu\text{m}/\mu\text{m}$) Delta- g_m
M_{1A}, M_{1B}	0.6/200	0.6/100
M_{1C}, M_{1D}	–	0.84/100
M_{2A}, M_{2B}	9.75/100	9.75/100
M_{3A}, M_{3B}	6/1	6/1
M_{4A}, M_{4B}	55/3	55/3
M_{5A}, M_{5B}	4/2	4/2
M_{6A}, M_{6B}	3/2	3/2
M_{7A}, M_{7B}	38/40	38/40
M_{8A}, M_{8B}	2/1	2/1

Table 3 Transconductor bias currents for $g_m = 4 \text{ nA/V}$

	VLPT- g_m	Delta- g_m
$I_{M_{1A}}$	1.7 nA	4.3 nA
$I_{M_{2A}}$	500 pA	500 pA
$I_{M_{4A}}$	1.2 nA	3.8 nA

**Fig. 6** Small-signal transconductance g_m as function of V_{in} and V_{TUNE}

$V_{TUNE} = 50 \text{ mV}$, for VLPT- g_m , a transconductance of 6.58 nA/V , a DC gain of 46.64 dB , a unity-gain frequency of 52.4 Hz and a phase error of 1.6° is found. For Delta- g_m , the respective values are 1.86 nA/V , 33.4 dB , 14.8 Hz and 1.06° . Figure 7 displays the input-referred noise spectral density for VLPT- g_m and Delta- g_m as function of V_{TUNE} . For $V_{TUNE} = 50 \text{ mV}$, these are $12.33 \mu\text{V}/\text{Hz}^{1/2}$ @ 1 Hz and $93.75 \mu\text{V}/\text{Hz}^{1/2}$ @ 1 Hz , for VLPT- g_m and Delta- g_m , respectively. As expected, due to its higher intrinsic transconductance, VLPT- g_m presents a lower noise figure than its counterpart Delta- g_m .

To finally implement the Wavelet Transform, one should be able to scale and shift in time (and, consequently

in frequency) the *gauss1* impulse response. As seen in Fig. 8, by changing the values of V_{TUNE} accordingly, different (dyadic) scales were implemented, while preserving the shape of the impulse response waveform. Figure 9 illustrates the frequency response of the same 4 dyadic scales with center frequencies ranging from 14 to 120 Hz for V_{TUNE} varying from 10 to 80 mV, for a wavelet filter implemented with ideal transconductors, VLPT- g_m and Delta- g_m , respectively. Figure 10 shows the total harmonic distortion (THD) of VLPT- g_m and Delta- g_m as a function of V_{TUNE} . As it can be observed, distortion is represented by $\text{THD} < -46 \text{ dB}$ over the range of $10 \text{ mV} < V_{TUNE} < 80 \text{ mV}$.

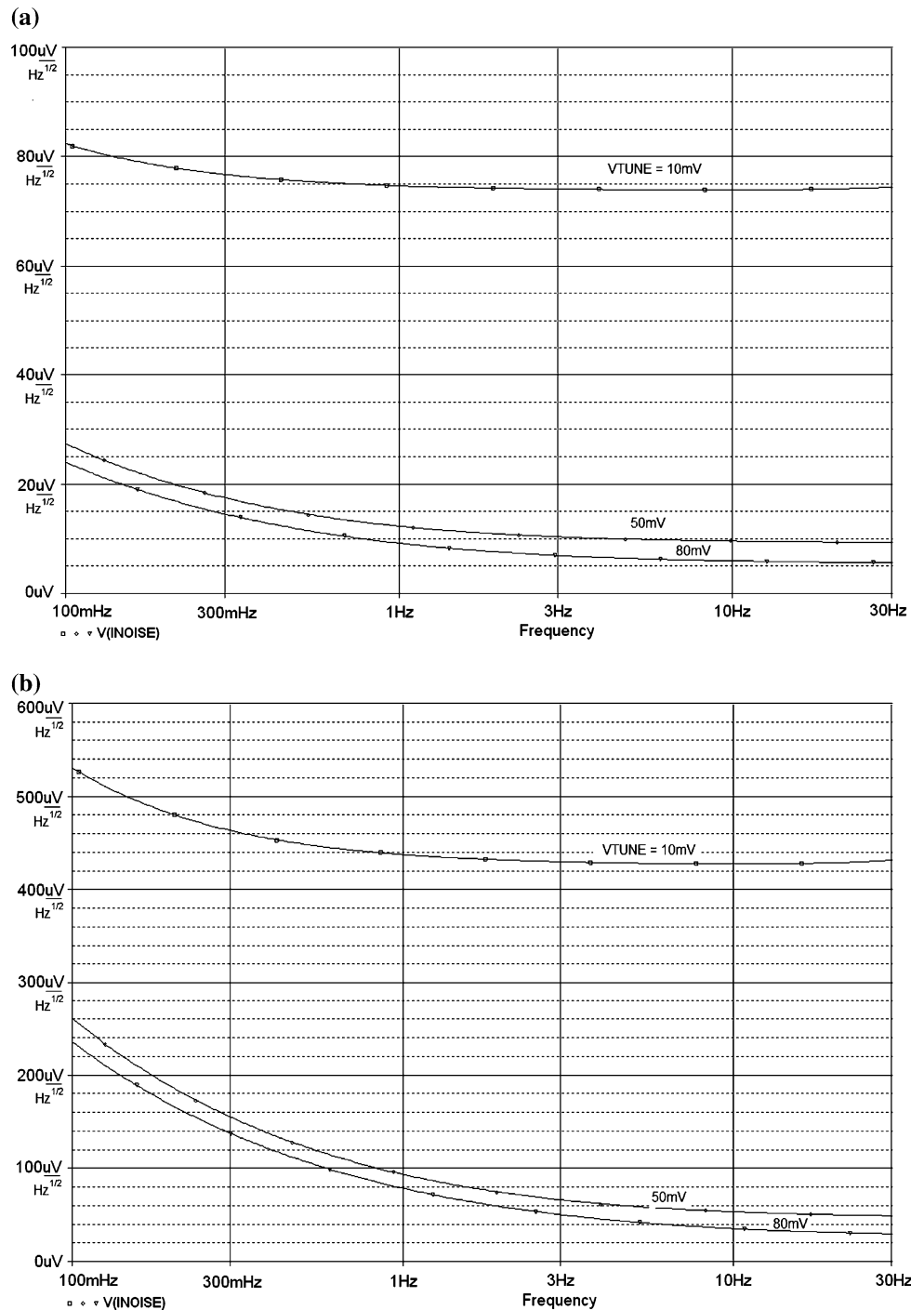
Monte Carlo analyses were also carried out to verify the dependence of g_m on mismatch and process parameters. A spread of 5% on both (W/L) and V_{T0} in input transistors revealed a maximum variation of 2.6% in the transconductance value for VLPT- g_m . Figure 11 shows the variation of g_m as function of Δ in Delta- g_m . One can clearly observe the trade-off between the absolute value of g_m and its precision. Offering a good compromise, a Delta- g_m transconductor with $\Delta = 0.4$ was selected to implement the wavelet filter.

Simulation results are summarized in Table 4. The total power consumption of Delta- g_m filter equals 114 nW , which is approximately twice the amount consumed by the same filter made up of VLPT- g_m transconductors. The input-referred noise is $156 \mu\text{V}/\sqrt{\text{Hz}}$ @ 1 Hz and $119 \mu\text{V}/\sqrt{\text{Hz}}$ @ 100 Hz for VLPT- g_m filter, whereas $642 \mu\text{V}/\sqrt{\text{Hz}}$ @ 1 Hz and $460 \mu\text{V}/\sqrt{\text{Hz}}$ @ 100 Hz for Delta- g_m filter. Both topologies present similar data for output resistance ($10^{10} - 10^{11} \Omega$) and harmonic distortion ($\text{THD} < 40 \text{ dB}$ @ $V_{in} = 200 \text{ mV}_{pp}$). With respect to VLPT- g_m , major advantages of Delta- g_m are its lower transconductance and larger bandwidth. For example, for $\Delta = 0.15$ (g_m variation around 5%), a minimum transconductance of 150 pA/V is achieved. For $\Delta = 0.4$ and $g_m = 1 \text{ nA/V}$, the cut-off frequency is 1.33 and 24 kHz for VLPT- g_m and Delta- g_m , respectively. Such an improvement in frequency response is due to the possibly smaller transistor sizes in Delta- g_m transconductors.

5 Conclusion

Two compact CMOS transconductors suitable for ultra-low power g_m -C filters operating in the Hz and sub-Hz range have been proposed. Their input transistors are kept in the triode-region to benefit from the lowest g_m/I_D ratio. To validate the circuit principle, these transconductors were employed as building blocks on a 6th-order L_2 approximated *gauss1* wavelet g_m -C filter.

Fig. 7 Input-referred noise spectral density for **(a)** VLPT- g_m and **(b)** Delta- g_m



The design was done anticipating realization in a standard $0.35\ \mu\text{m}$ n-well CMOS process and operation from a supply voltage V_{DD} of 1.5 V. Simulation data of electrical performance were obtained with Bsim3v3 models. For the VLPT- g_m filter, the transconductance ranges from 1 to 12 nA/V. Its overall power consumption equals 51 nW, for a total capacitance of 120 pF. For the Delta- g_m filter, the transconductance spans from 400 pA/V to 4.8 nA/V, with a power consumption of 114 nW, for a total capacitance of 48 pF. For

$V_{TUNE} = 50\ \text{mV}$, input-referred noise spectral density were $12.33\ \mu\text{V}/\text{Hz}^{1/2}$ @ 1 Hz and $93.75\ \mu\text{V}/\text{Hz}^{1/2}$ @ 1 Hz, for VLPT- g_m and Delta- g_m , respectively. In both circuits, THD was kept below 1% for signal swings up to $200\ \text{mV}_{pp}$.

The simulated impulse response of 6th-order wavelet filter differs only slightly from the ideal 6th-order impulse response for both topologies. From this, one may conclude that the coefficients have been implemented successfully. Owing to their ultra low-power consumption and

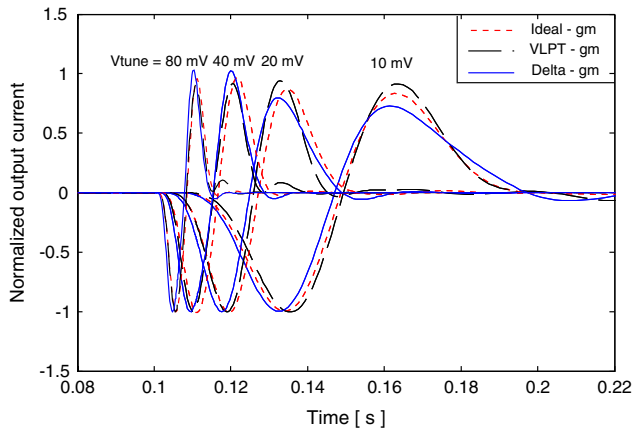


Fig. 8 Simulated impulse responses of the wavelet filter

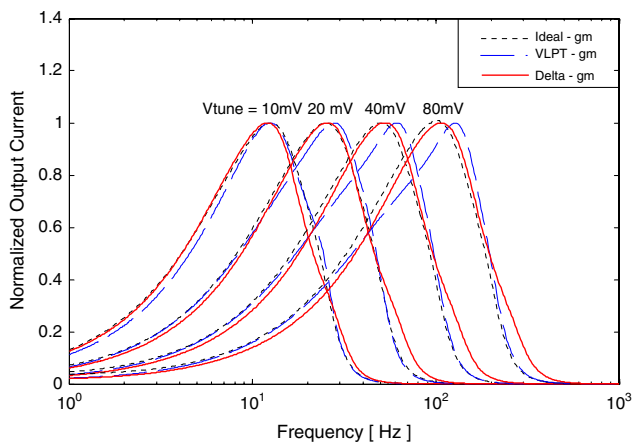


Fig. 9 Simulated frequency responses (magnitude) of the wavelet filter

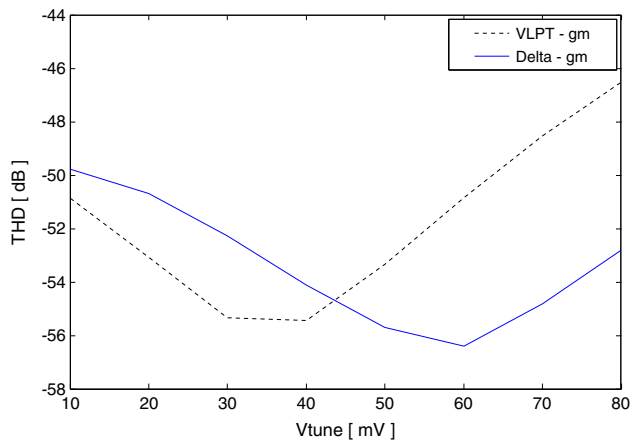


Fig. 10 Wavelet filter THD values obtained for distinct values of V_{TUNE}

compactness, the wavelet filter based on the proposed triode-transconductors becomes an attractive option to process very-low frequency signals in battery-operated systems, such as those required in biomedical devices.

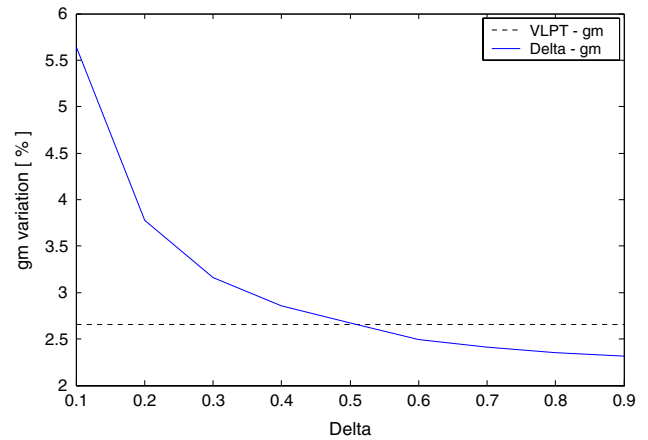


Fig. 11 Simulation (Monte Carlo analysis) result showing the variation of g_m as a function of Δ for the Delta- g_m , compared with the variation of g_m for the VLPT- g_m

Table 4 Summary of simulated results

	VLPT- g_m	Delta- g_m
Filter power (nW)	51	114
g_m bandwidth (kHz), $\Delta = 0.4$	1.33	24
Input eq. noise @ 1 Hz ($\mu V/\sqrt{Hz}$)	156	642
Input eq. noise @ 100 Hz ($\mu V/\sqrt{Hz}$)	119	460
Minimum g_m (nA/V)	$\cong 1$	$\cong 0.15$
R_{out} @ $g_m = 2$ nA/V (Ω)	1×10^{11}	4×10^{10}
g_m variation (%), $\Delta = 0.4$	2.7	2.9
g_m variation (%), $\Delta = 0.15$	2.7	5
THD (dB), $V_{TUNE} = 20$ mV, $V_{IN} = 150$ mV _{pp}	-53	-51
THD (dB), $V_{TUNE} = 80$ mV, $V_{IN} = 150$ mV _{pp}	-47	-53

References

1. Veeravalli, A., Sánchez-Sinencio, E., & Silva-Martínez, J. (2002). Transconductance amplifier structures with very small transconductances: A comparative design approach. *IEEE JSSC*, 37(6), 770–775.
2. Silva-Martínez, J., & Salcedo-Suner, J. (1997). IC voltage to current transducers with very small transconductances. *Analog Integrated Circuits and Signal Processing*, 13, 285–293. doi:10.1023/A:1008286718560.
3. Steyaert, M., Kinget, P., Sansen, W., & Van Der Spiegel, J. (1991). Full integration of extremely large time constants in CMOS. *Electronics Letters*, 27(10), 790–791. doi:10.1049/el:19910495.
4. Arnaud, A., & Galup-Montoro, C. (2004). A fully integrated 0.5–7 Hz CMOS bandpass amplifier. *Proceedings of IEEE ISCAS*, 1, pp. 445–448, Vancouver, Canada.
5. Veeravalli, A., Sánchez-Sinencio, E., & Silva-Martínez, J. (2002). A CMOS transconductance amplifier architecture with wide tuning range for very low frequency applications. *IEEE JSSC*, 37(6), 776–781.

6. Pennock, J. (1985). CMOS triode transconductor for continuous-time active integrated filters. *Electronics Letters*, 21(18), 817–818. doi:10.1049/el:19850576.
7. De Lima, J. A., & Dualibe, C. (2001). A linearly-tunable CMOS transconductor with improved common-mode stability and its application to gm-C filters. *IEEE TCAS-II*, 48(7), 649–660.
8. De Lima, J. A., & Serdijn, W. A. (2005). A compact nA/V CMOS triode-transconductor and its application to very-low frequency filters. *Proceedings of IEEE ISCAS*, Kobe.
9. De Lima, J. A., & Serdijn, W. A. (2005). Compact nA/V triode-MOSFET transconductor. *Electronics Letters*, 41, 1113–1114. doi:10.1049/el:20052551.
10. Haddad, S. A. P., Bagga, S., & Serdijn, W. A. (2005). Log-domain wavelet bases. *IEEE TCAS-I*, 52(10), 2023–2032.
11. Bruschi, P., Barillaro, G., Piere, F., & Piotta, M. (2004). Temperature stabilized tunable Gm-C filter for very low frequencies. *Proceedings of ESSCIRC*, Sept. 21–23, pp. 107–110.
12. Karel, J. M. H., Peeters, R. L. M., Westra, R. L., Haddad, S. A. P., & Serdijn, W. A. (2005). Wavelet approximation for implementation in dynamic translinear circuits. *Proceedings of IFAC World Congress 2005*, Prague, July 4–8.



Peterson R. Agostinho was born in Taubaté, Brazil, on January 22, 1980. He received his B.S. Degree in Electrical Engineering from the State University of São Paulo (UNESP), Brazil, in 2003, and the M.S. degree from University of Campinas (UNICAMP), Brazil, in 2006. In July 2006 he joined Technological Institute of Aeronautics to developing his Ph.D. program. He is currently involved in the development of high performance analog circuits for aerospace applications.



Sandro A. P. Haddad was born in Anapolis, Brazil, on February 8, 1977. He received his B.S. Degree in Electrical Engineering from the University of Brasilia (UnB), Brazil, in 2000, with honors. He was awarded the best-graduated student of the year, from the Faculty of Electrical Engineering, UnB. In February 2001, he joined the Electronics Research laboratory, Delft University of Technology (TUDelft), The Netherlands,

where he started research towards his Ph.D. degree. His project was part of BioSens (Biomedical Signal Processing Platform for Low-Power Real-Time Sensing of Cardiac Signals). His research interests included low-voltage, ultra low-power analog electronics and biomedical systems, and high-frequency analog integrated circuits for UWB communications. He received his Ph.D. degree in December 2006, with the thesis entitled “Ultra Low-Power Biomedical Signal

Processing – An Analog Wavelet Filter Approach for Pacemakers”. In January 2007 he joined Freescale Semiconductor as Analog IC Designer.



Jader A. De Lima obtained both B.S. ('77) and M.S. ('80) degrees in Electrical Engineering from Universidade de São Paulo, Brazil, and his Ph.D. degree ('84) in Electrical Engineering from Universidade Estadual de Campinas, Brazil. Research Assistant at the University of Edinburgh, U.K., from 1986 to 1989. He joined then Motorola (EDO), in Geneva, Switzerland and FASELEC/Philips in Zurich, Switzerland. From

1992 to 1995 he was a design leader at the Microcontroller Group of Thomson Consumer Electronic Components, in Grenoble, France. He was an Associate Professor at Universidade Estadual Paulista (UNESP), in Brazil, from 1994 to 2004. Currently, he is a Design Manager at Freescale Semiconductor, in Campinas, Brazil. His main interests are low-voltage low-power analogue design, power management, continuous-time filters and biomedical instrumentation.



Wouter A. Serdijn was born in Zoetermeer ('Sweet Lake City'), the Netherlands, in 1966. He started his course at the Faculty of Electrical Engineering at the Delft University of Technology in 1984, and received his 'ingenieurs' (M.Sc.) degree in 1989. Subsequently, he joined the Electronics Research Laboratory of the same university where he received his Ph.D. in 1994. His research interests include low-voltage, ultra-low-power, high-

frequency and dynamic-translinear analog integrated circuits along with circuits for RF and UWB wireless communications, cochlear implants, portable, wearable, implantable and injectable ExG recorders and pacemakers. Dr. Serdijn is co-editor and co-author of the books *Power Aware Architecting for Data Dominated Applications* (Springer, 2007), *Adaptive Low-Power Circuits for Wireless Communications* (Springer, 2006), *Research Perspectives on Dynamic Translinear and Log-Domain Circuits* (Kluwer Academic Publishers, Boston, 2000), *Dynamic Translinear and Log-Domain Circuits* (Kluwer Academic Publishers, Boston, 1998) and *Low-Voltage Low-Power Analog Integrated Circuits* (Kluwer Academic Publishers, Boston, 1995). He authored and co-authored more than 200 publications and presentations. He teaches *Analog Electronics*, *Analog Signal Processing*, *Micropower Analog IC Design* and *Electronic Design Techniques*. In 2001 and 2004, he received the EE Best Teacher Award.